Master's Thesis

A Study on the Design Conditions of NP Ratio according to the Operating Temperature of Lithium-ion Battery

Jaehyun An

School of Energy and Chemical Engineering
(Battery Science and Technology)

Ulsan National Institute of Science and Technology

2021

A Study on the Design Conditions of NP Ratio according to the Operating Temperature of Lithium-ion Battery

Jaehyun An

School of Energy and Chemical Engineering
(Battery Science and Technology)

Ulsan National Institute of Science and Technology

A Study on the Design Conditions of NP Ratio according to the Operating Temperature of Lithium-ion Battery

A thesis/dissertation submitted to
Ulsan National Institute of Science and Technology
in partial fulfillment of the
requirements for the degree of
Master of Science

Jaehyun An

12/22/2020

Approved by

Advisor
Kyeong-Min Jeong

A Study on the Design Conditions of NP Ratio according to the Operating Temperature of Lithium-ion Battery

Jaehyun An

This certifies that the thesis/dissertation of Jaehyun An is approved.

12/22/2020

Advisor: Kyeong-Min Jeong

Hyun-Kon Song

Dong-Hwa Seo

Abstract

In this study, in preparation for diversification of applications, the results of the half-cell formation cycles at 25℃ and 40℃ were compared to see how temperature changes affect the reversible specific capacity and initial Coulombic efficiency of active materials. And, a three-electrode system with a reference electrode was used for accurate potential measurement.

For more accurate full cell capacity prediction, the cathode and anode limit design was applied. And the accuracy of the design is verified through the voltage behavior of the cathode and anode using a three-electrode system.

Based on the results of the half-cell formation cycle at 25℃ and 40℃, respectively, the process of designing a full cell and predicting capacity was dealt with. And it was studied how the difference between design temperature and operating temperature affects the full cell.

Contents

List of Figures

List of Tables

I. Introduction

1.1 Application of lithium-ion battery

Due to its attractive properties including high energy efficiency, lack of memory effect, long cycle life, high energy density and high power density, the application of lithium-ion batteries is diversifying. (**Fig. 1**)[1] In 1991, Sony started producing the first product using LiCoO2 as a cathode active material, graphite as anode graphite. Today, it is used in consumer electronics and devices such as smartphones, lab tops, power tools, grid energy and industry such as ESS, and transportation such as EV.

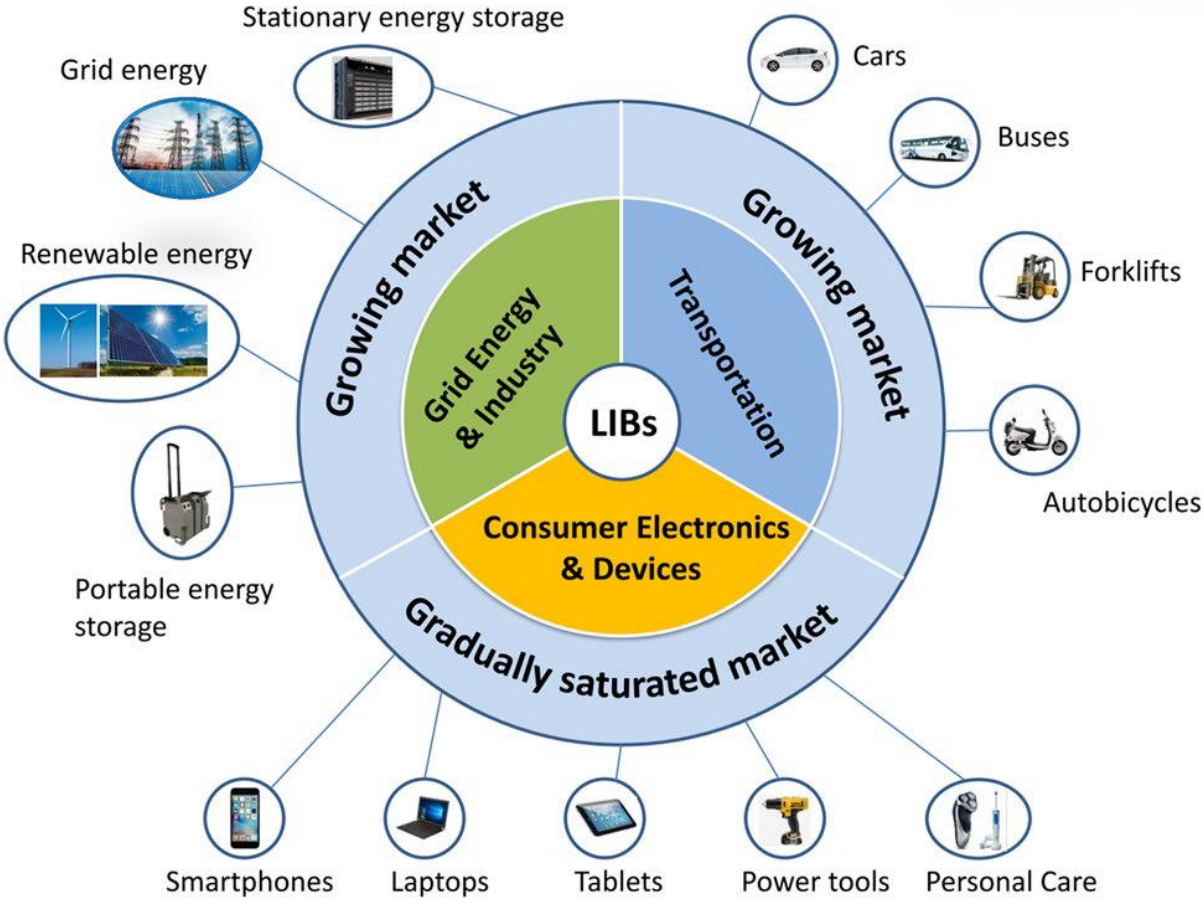

Figure 1. Applications of LIBs in the three main fields including consumer electronics and devices, transportation, as well as grid energy and industry

1.2 Design of lithium-ion battery

1.2.1 Practical design of lithium-ion battery

The diversification of lithium-ion battery applications is because it can meet the requirements of applications as an energy storage medium. LIB is used in various places such as a battery of a power tool that requires high power characteristics through various design conditions, and a mobile phone by extending the usage time with high energy density. As such, the design of lithium-ion batteries is designed to meet the requirements of the application.

The practical design of lithium-ion batteries starts with the requirements of the application. (**Fig. 2**) They are designed to meet their requirements such as form factor (size, density, dimension, …) and performance (power density, energy density, cycle life, run time, ….). To meet the requirements, it starts with the selection of the four major components of lib: cathode, anode active material, separator, and electrolyte.

To meet the voltage one of the requirements, first of all, it is necessary to select a pair of active material that achieves the voltage condition. If the selection of active materials is complete, the next is a selection of separators and electrolytes that are electrochemically stable in their voltage range and can improve performance. The separator serves to physically separate the cathode and anode, and it must be able to withstand physical stress such as dendrite generated at the anode. However, if the thickness is increased for strength, the energy density decreases as much, so it must be selected and designed in consideration of the performances. The electrolyte containing li+-ion, which plays a role in charge transfer of lithium-ion batteries, requires the choice of salt type and concentration, solvent composition, and additives that help to form a good SEI film.

With these selected materials, an electrochemical evaluation of the active material is made. The reversible specific capacity of active material can be measured through the half-cell test. The design of the full cell proceeds through the measured reversible specific capacity of active material. NP ratio design, which is the capacity ratio of anode and cathode, is also made at this stage.

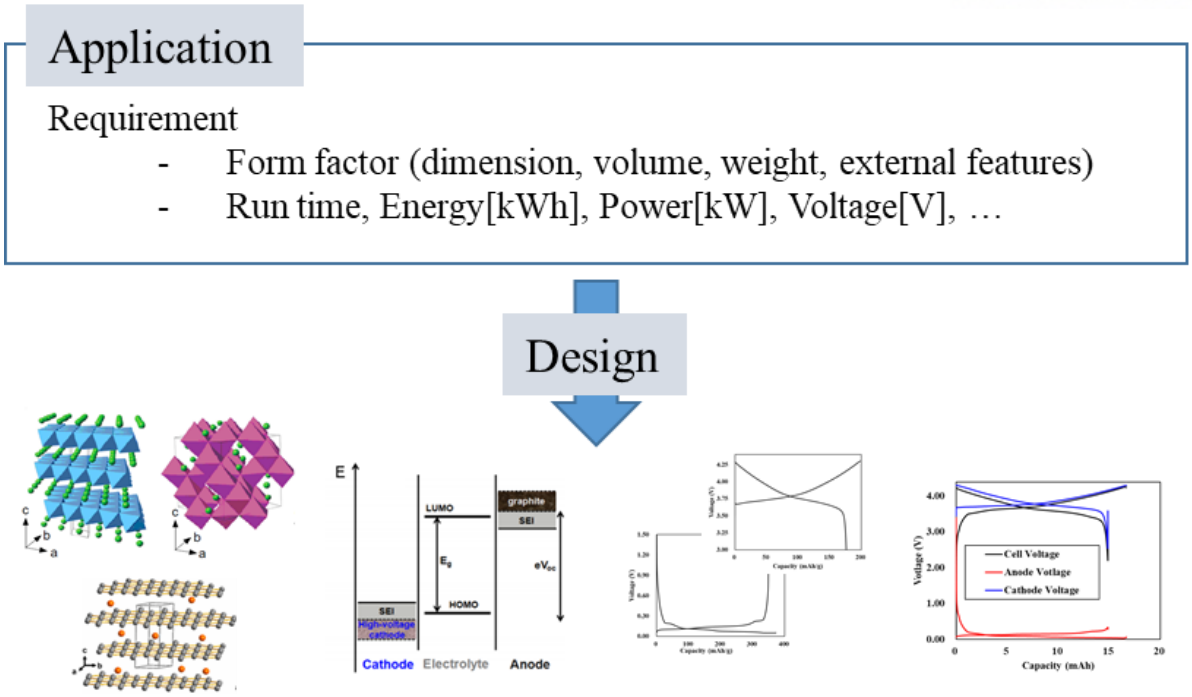

Figure 2. Practical design process of lithium-ion battery cell

1.2.2 Full cell design using new active material

Unlike practical design, the design in this study is for the introduction of new active material. When new active materials are developed, they first need to be analyzed electrochemically. The setting of the usable voltage range, measurement of specific capacity through charging/discharging, and measurement of irreversible capacity are in progress. When designing a full cell as a result of the electrochemical evaluation of the active material, the voltage range of the full cell can be determined by reflecting the voltage range of the new active material. The following steps are similar to the practical design process.

1.2.3 Design factor of lithium-ion battery

The design process of a lithium-ion battery was mentioned before. In the process of designing a product to satisfy the requirements of the application, it is necessary to determine various parameters. It can be largely classified into physical, chemical, and electrochemical properties.[2] In order to control each parameter, the electrode should be designed in consideration of the physical properties of the electrode such as loading level, composite density, etc., and the interaction factor with the electrolyte.

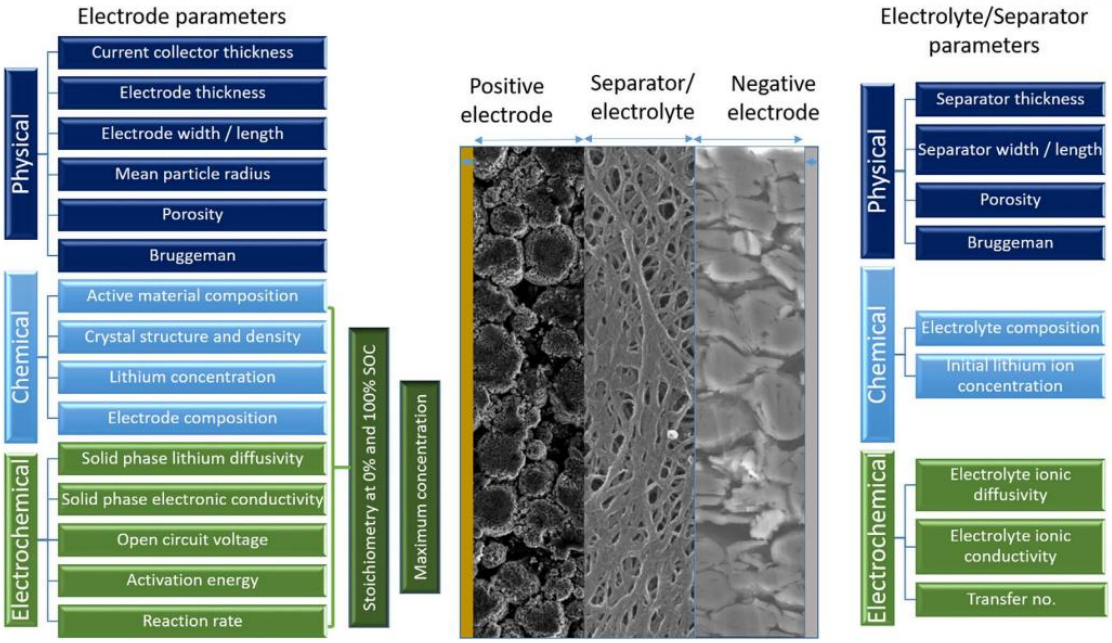

Figure 3. Summary of the parameterization requirements and physical, chemical, and electrochemical property elucidation

1.2.4 Environmental condition of lithium-ion battery

Environmental factors that directly affect the aforementioned parameters must also be reflected in the cell design. One of them is temperature. It is important to manage the temperature at which the cell is stored and the heat generated when the lithium-ion battery is charged or discharged.

II. Experimental

2.1 Electrode and cell fabrication

Table 1. was filled with information on cathode, anode materials. LiNi0.6Co0.2Mn0.2O2(NCM622, HX12Th, Umicore) was used as the cathode active material. PVdF and carbon black were used as a binder and conductive additive respectively. The composite ratio of the electrode was 96 : 2 : 2 (NCM622 : PVdF : Super P). Graphite was used as the anode active material. CMC and SBR were used as a binder. Composite ratio of electrode was 97.4 : 1.2 : 1.4 (Graphite : CMC : SBR).

The cathode slurry was mixed by homogenizer (ED-1, NISSEI, Japan) under 10000 rpm for 1 hour. And cathode slurry was coated on an aluminum current collector with a loading level of 16-17 mg/cm2. The cathode was calendered until the composite density became 3.3 g/cc. The anode slurry was mixed by homogenizer under 12000 rpm for 1 hour. And anode slurry was coated on a copper current collector with a loading level of 9-10 mg/cm2. The anode was calendered until the composite density became 1.6 g/cc.

The cathode was charged to 4.3V under CC/CV (constant current/constant voltage) condition at half-cell, discharged to 2.7V under CC condition. The anode was charged to 0.05V under CC/CV condition at half-cell, discharged to 1.5V under CC condition.

1.0 M LiPF6 in EC/EMC/DEC=25/45/30 (v/v) + 1 wt.% VC + 3 wt.% FEC was used as a electrolyte. And PE separator (SK Inno.) was used.

Fig 4. is a configuration of the pouch cell. The reference electro was used for a three-electrode cell system. **Table 2.** is filled with dimension information of the pouch cell. The anode was larger than the cathode. This is to avoid dendrite generation by overloading the current density at the edge of the electrode. The separator used two sheets to place the reference electrode between the electrode and the electrode.

Table 1. Materials and experimental conditions.

	Cathode	Anode
Active material	NCM 622 HX12Th, Umicore	Graphite S350, Timcal
Binder	Polyvinylidene fluoride (PVdF) KF#9300, Kureha	Carboxymethyl cellulose (CMC) MAC350LC, Zeon Styrene-butadiene rubber (SBR) BM-451B, Zeon
Solvent	N-Methyl-2-pyrrolidone (NMP) Samchun	Di water
Conductive additive	Carbon black Super P, Timcal	-
Composite ratio	96 : 2 : 2 (AM : Binder : C.A.)	97.4 : 1.2 : 1.4 (AM : CMC : SBR)
Current collector	Aluminum (30 um)	Copper(20 um)
Loading level	16-18 mg/cm^2	9-10 mg/cm^2
Composite density	3.3 g/cm^3	1.6 g/cm^3
V range	4.3V - 2.7V	0.05V - 1.5V
Electrolyte	1.0 M $LiPF_6$ in EC/EMC/DEC=25/45/30 (v/v) + 1 wt.% VC + 3 wt.% FEC	
Separator	PE, SK Innovation	

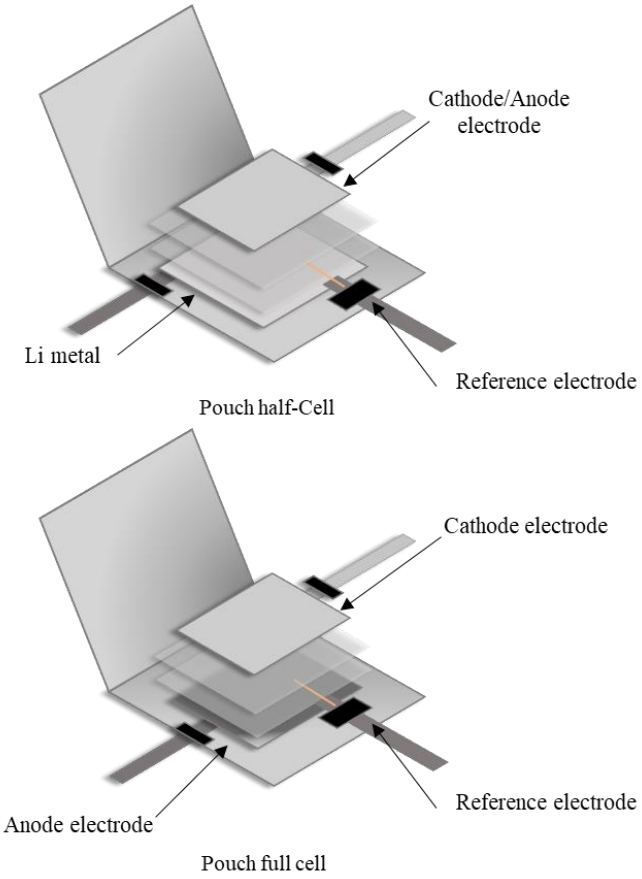

Figure 4. Pouch cell configuration

Table 2. Dimension of pouch cell

	Dimension	remarked
Cathode	20 * 25 mm^2	Al tab.
Anode	22 * 27 mm^2	Ni tab.
Separator	26 * 30 mm^2, t : 19.2 um	2 separators
Reference electrode	D : 100 μm, l : 15 mm (Cu wire)	Between 2 separators
Lithium metal	30 * 30 mm^2 , t : 200 μm	Half-cell
Pouch	50 * 50 mm^2 (folded)	

2.2 Three-electrode system

2.2.1 Reference electrode

In order to measure the accurate specific capacity, an accurate voltage measurement is required. For the design of a full cell, the specific capacity of the cathode and anode active material is measured through a half-cell using Li metal through control of the voltage range. However, in the case of a two-electrode system using Li metal, the exact potential of the working electrode cannot be measured due to the impedance of the Li metal. Not an accurate measure of the potential means that the specific capacity cannot be accurately measured. Thus, in this study, the three-electrode system by using the reference electrode was applied for accurate measurement of anode and cathode active material's specific capacity.

In addition to the measurement of accurate specific capacity, the use of a reference electrode can confirm the voltage behavior and contribution of the positive and negative electrodes in the full cell. Understanding the behavior of the anode and cathode in a full cell leads to an understanding of the voltage behavior of a full cell. Within the voltage range set to use a full cell, it is possible to know which electrode acts as the main when the charge and discharge cut-off condition is reached. At the end of the charge state, the charge state of each electrode can also be determined through the potential of the cathode and anode electrodes. This makes it possible to know which degradation occurred in which electrode when degradation occurred in a full cell.

Fig 5. shows two reference electrodes compared to be introduced in this study. The biggest difference between the two electrodes is the location of the reference electrode. **Fig 5.(a)** is located outside the reacting area where the electrode is facing, and **Fig 5.(b)** is located on the facing surface. And the shape of the reference electrode is also different. Since **Fig 5.(b)** is located in the reacting area and can interfere with the reaction, a microreference electrode in which lithium is deposited on the Cu wire was used.[3]

For comparison and selection of the two electrodes, the results of the formation cycle of half-cell and full cell were compared.

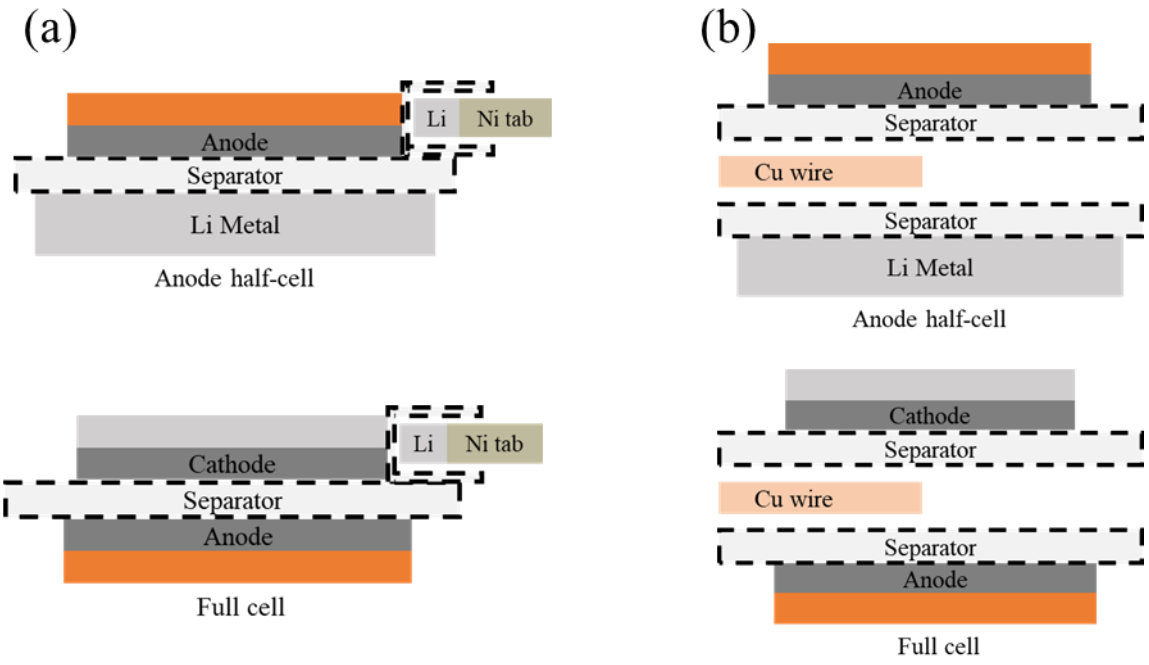

Figure 5. Three-electrode pouch cell cross-section configuration with (a). Ni tab, (b) Cu wire.

It is possible to determine which electrode is measuring more accurately through the measured voltage graph. **Fig 6.(a), (c)** shows anode half-cell result. The anode half-cell was charged to 0.05V under CC/CV condition with 0.1C rate. When comparing the CC capacity of the two cells (a) and (c), the cell using the Ni tab showed a lower capacity than that of the Cu wire. This is because the potential which was measured by Ni tab reference reached the cut-off voltage first, and this is the effect of overpotential due to the distance between the reference electrode and the working electrode when measuring the potential.

Both full cells were designed with similar NP ratios. If the accuracy of the electric potential measurement of the two reference electrodes is similar, since it is a full cell with a similar NP ratio, a similar electric potential should be measured at the end of the charge. But at the end of the charge, it can be seen that the anode potential measured using the Ni tab is higher than that of the Cu wire. When predicting the anode potential according to the charging capacity of the anode, it can be determined that 0.06V measured by the Cu wire is more accurate. Thus, in my three-electrode system, the Cu wire reference electrode which locates between the working and the counter electrode was used as the reference electrode.

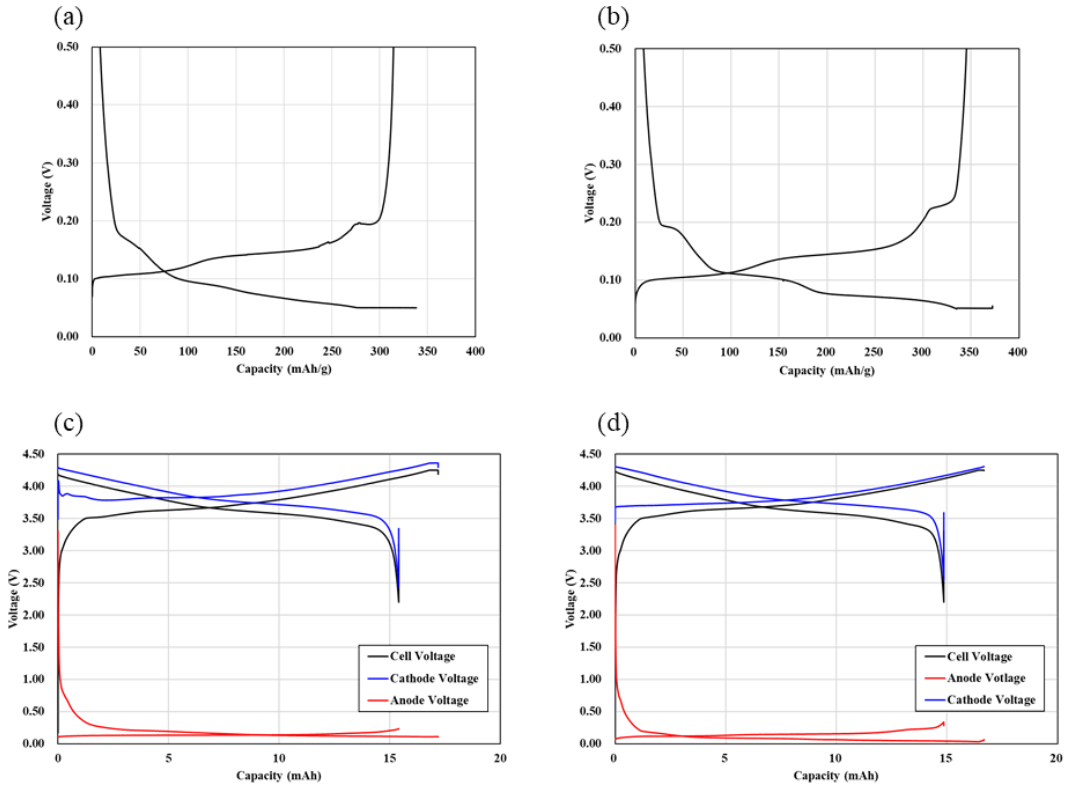

Figure 6 Anode half-cell formation cycle with (a) Ni tab, (b) Cu wire, and Full cell formation cycle with (c) Ni tab, (d) Cu wire.

Table 3. Anode half-cell formation cycle with three-electrode system

Reference electrode	Specific CC charge capacity (mAh/g)	Specific CC/CV charge capacity (mAh/g)	Specific Discharge capacity (mAh/g)	ICE
Ni tab.	280.2	338.2	316.6	93.6%
Cu wire	332.3	373.0	350.8	94.1%

Table 4. Anode and cathode potential in full cell at the end of the charge

Reference electrode	Cell (V)	Cathode (V)	Anode (V)
Ni tab.	4.25	4.36	0.11
Cu wire	4.25	4.31	0.06

III.Results and discussion

3.1 Half-cell test result at 25℃

Table 5. shows the specific capacity of the anode and cathode half-cell test at 25℃. Charging for both cathode (NCM622) and anode (NCM622) was evaluated by the constant current/constant voltage (CC/CV) method. The charging capacity up to the cc section of the cathode is 197.9 mAh/g, and the charging capacity of the CC/CV method is 198.9 mAh/g. On the other hand, the CC and CC/CV charging capacities of the anode are 327.8 mAh/g and 372.4 mAh/g, respectively, which is larger than that of the cathode. In the initial Coulombic efficiency, the anode was also higher than that of the cathode. And both sides showed a steep voltage change behavior at the end of the discharge.

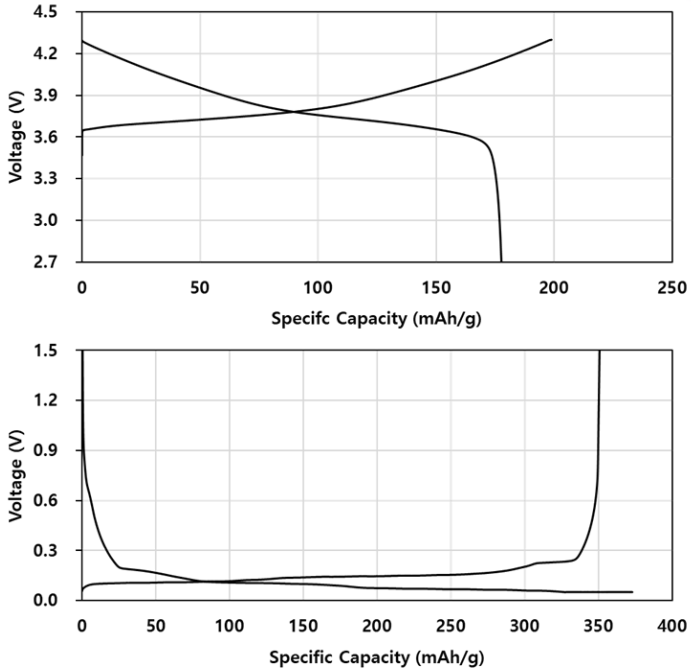

Figure 7. Formation cycle of NCM622, Graphite half-cell graph at 25℃

Table 5. Cathode, anode half-cell formation cycle result

	Cathode 25℃	Anode 25℃
Specific charge capacity (CC / CC-CV) (mAh/g)	197.9/198.9	327.8/372.4
Specific discharge capacity (mah/g)	177.6	350.0
Initial Coulombic efficiency (ICE)	89.3%	94.0%

3.2 NP ratio design at 25℃

Through the half-cell result, we can predict the reversible capacity and ICE of the full cell. For the convenience of predicting the voltage behavior of the full cell and comparing the results with the results, the target NP ratio of the full cell was designed with the CC charge capacity ratio close to 1.0. It has a higher capacity margin of anode compared to commercially available products. Since the charge capacity ratio of the CC section of the target NP ratio was close to 1.0, the charge cut off voltage of the full cell was determined to be 4.25 V, the difference between the charge cut-off voltages of the positive and negative half-cells, and the discharge cut-off voltage Was determined to be 2.2V, which is the difference between 3.0V and 0.8V, which is the voltage of the section in which the cathode and anode active materials are sufficiently discharged.

Fig. 8 is a graph showing the prediction of the full cell voltage curve through the half-cell result. At the end of the discharge, it can be seen that the potential of the full cell decreases rapidly and reaches the cut-off. The main reason for this is that the potential of the cathode has decreased rapidly. The low efficiency of the cathode allows the discharge of the full cell to be completed even if residual lithium remains in the anode in the full cell. A case in which discharge is completed by the cathode and capacity prediction is possible can be called a cathode limit design cell.

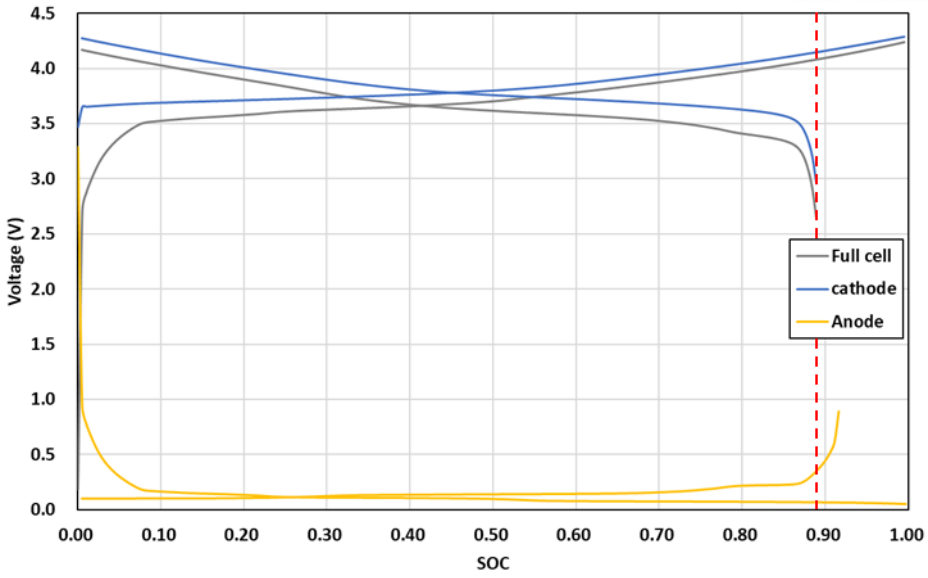

Figure 8. Predicted full cell plot through half-cell result at 25℃

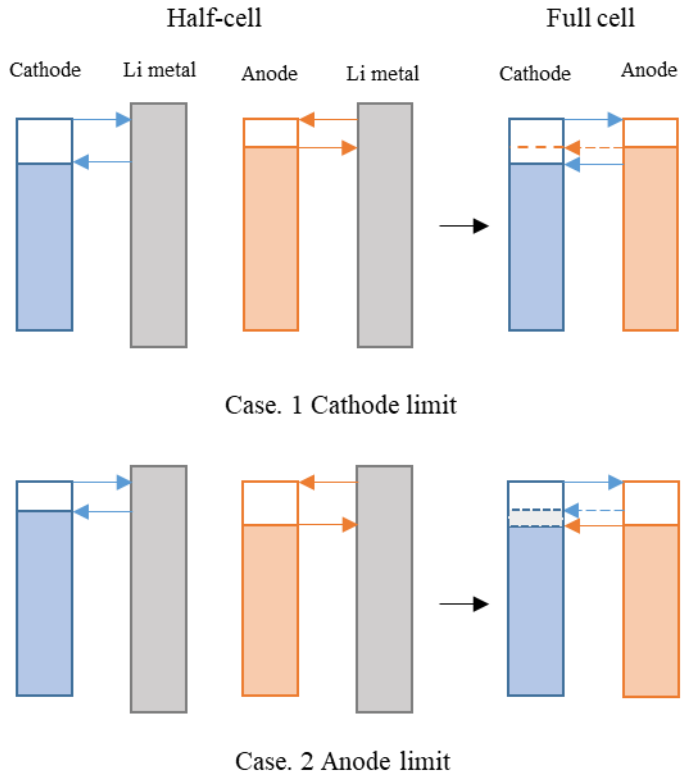

Figure 9. Schematic diagram of limit design of full cell

3.2.1 Cathode limit design

The two limitation types are distinguished by which electrode causes the termination of the discharge step during galvanostatic cycling in the full cell.[4] **Fig. 9** is a schematic diagram showing two cases of limit design of the full cell through the result of the half-cell in the design process of full cell. The bar in the figure shows only the operating voltage range of the half-cell test. (Cathode: 4.3V-2.7V, Anode: 0.05V-1.5V) There are three causes of the specific reverse capacity of the formation cycle of the cathode active material. (1) excess charge capacity caused by irreversible reactions with electrolyte, (2) loss of active material due to irreversible structural changes, particularly on the surface, which could include the formation of an SEI-type later, and (3) slow kinetics for lithium intercalation.[5] The schematic diagram shows irreversible capacity due to bad kinetics due to changes in structure and site disappeared by cation mixing that occurred with charging. The irreversible capacity of the formation cycle of the anode is due to SEI generation, and the figure shows that the discharge specific capacity is the charge capacity excluding Li-ions used for SEI generation.

Fig. 9 Case 1. showed that the site limitation of the positive electrode is greater than the irreversible capacity caused by SEI generation in the negative electrode. Due to the site limitation of the cathode at the end of the discharge, the potential of the cathode decreases sharply, and the voltage of the full cell decreases to complete the discharge.

3.2.2 Anode limit design

Fig 9. Case 2. is a case where the li ions used to create the SEI layer of the cathode are more than sites that cannot be used in the cathode. This is the case where the anode potential rises due to exhaustion of the inventory of lithium ions held by the cathode before the site limitation of the cathode occurs. This is the case where the increase in anode potential at the end of discharge is the main factor that terminates the discharge of the full cell.

The anode limiting and cathode limiting designs are each determined by the material and can be determined by the active material mass ratio (NP ratio).

3.2.3 NP ratio design at 25℃

Fig 10. shows the results of the formation cycle at 25℃ for the cell designed at 25℃. And **Table 6.** was filled with design NP ratios. **Table 7.** was filled with the result of the formation cycle. As expected, it was confirmed that the potential drop due to the decrease in the kinetic end of the discharge of the cathode electrode is the main cause of the decrease in the discharge voltage of the full cell, and the design of the cathode limit is accurate. When comparing the design predicted value and the result, both the charging and discharging capacity of the result showed slightly larger values. However, the efficiency was similar to the predicted value.

The reason why the charging capacity of the full cell is greater than that of the design can be seen through at the end of the charge cathode potential of the full cell. **Fig 11.** is the cell voltage and cathode potential at the end of the charge. Although the charge cut-off voltage of the cathode used in the design is 4.3V, it can be seen that charging is terminated at a higher voltage as 4.32V in the actual full cell. The reason for this is that charging is completed at a potential higher than the design expected due to the large area of the anode compared to the cathode.

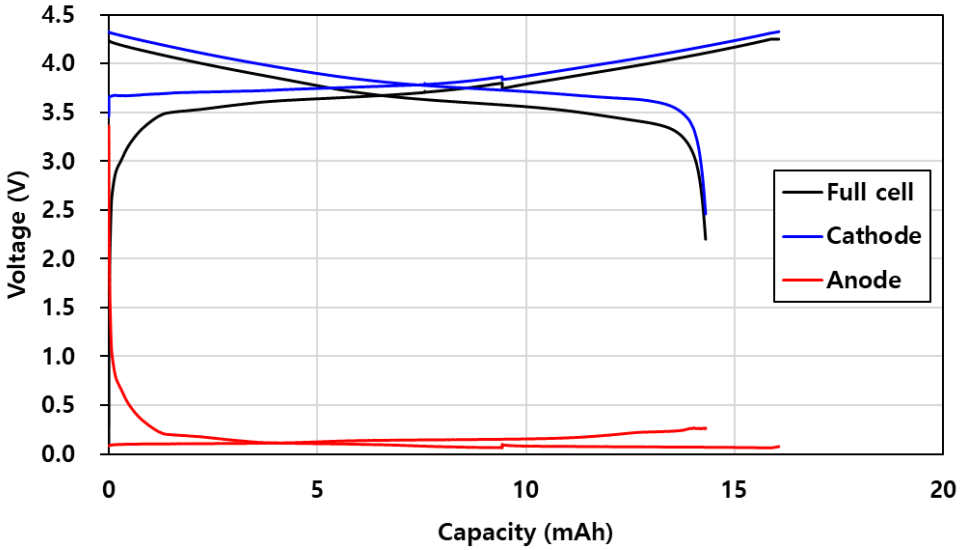

Figure 10. Formation cycle graph of NCM62/Graphite full cell operated at 25℃

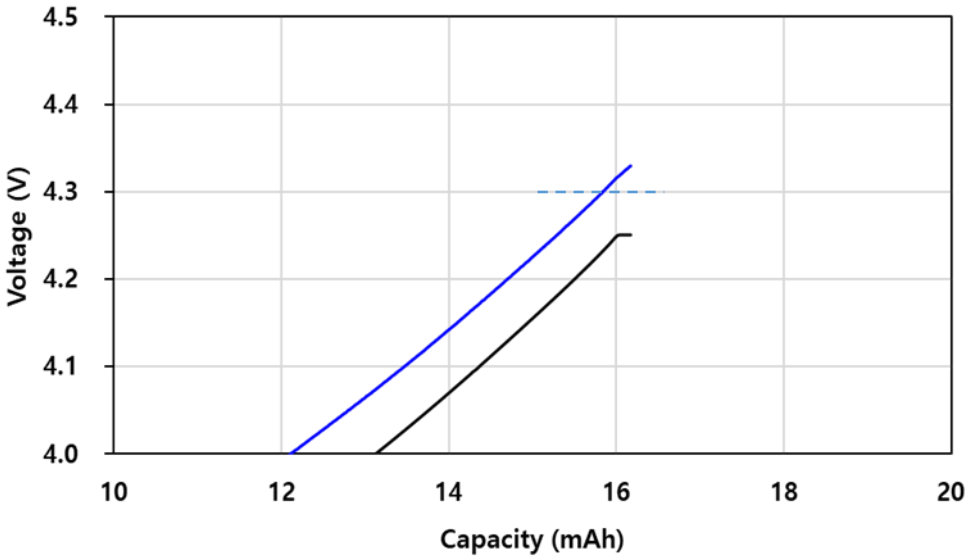

Figure 11. Formation cycle graph at the end of the charge of NCM622/Graphite full cell operated at 25℃

Table 6. NP ratio design of full cell at 25℃

	CC Charge NP	Charge NP	Discharge NP
Design	1.020	1.155	1.216

Table 7. Full cell formation cycle result at 25℃

	Charge capacity (mAh)	Discharge capacity (mAh)	ICE
Design	15.80	14.11	89.3%
Real	16.06	14.31	89.1%

3.3 Half-cell test result at 40℃

The operating temperature can affect each electrode. When the operating temperature increased from 25℃ to 40℃, the change of the reversible specific capacity and ICE of each active material was observed through the 40℃ formation cycle. **Fig 11.** and **Table 9.** are the result of the formation cycle test at 40℃. The specific charge capacity of the cathode did not show a big difference between 25℃ and 40℃, but it can be seen that ICE increased to 92.3% as the specific discharge capacity increased 7.1mAh/g at 40℃. Discharge capacity increased thanks to facilitating the kinetics with increasing temperature. Kasnatscheew, et al. studied that the effect of kinetic limitations during the lithiation process can be quantified by applying the electrostatic potential (CP) step after discharge.[6]

The specific capacity of the cathode increased both charge and discharge. However, compared to the increase in charge, the increase in discharge was lower and the ICE was lowered. This is because SEI production increased more due to the increase in the reaction rate due to the increase in temperature. As the temperature increases, the Li diffusion rate increases at the surface, and the facilitating of the reaction driving force promotes the formation of the SEI layer.[7]

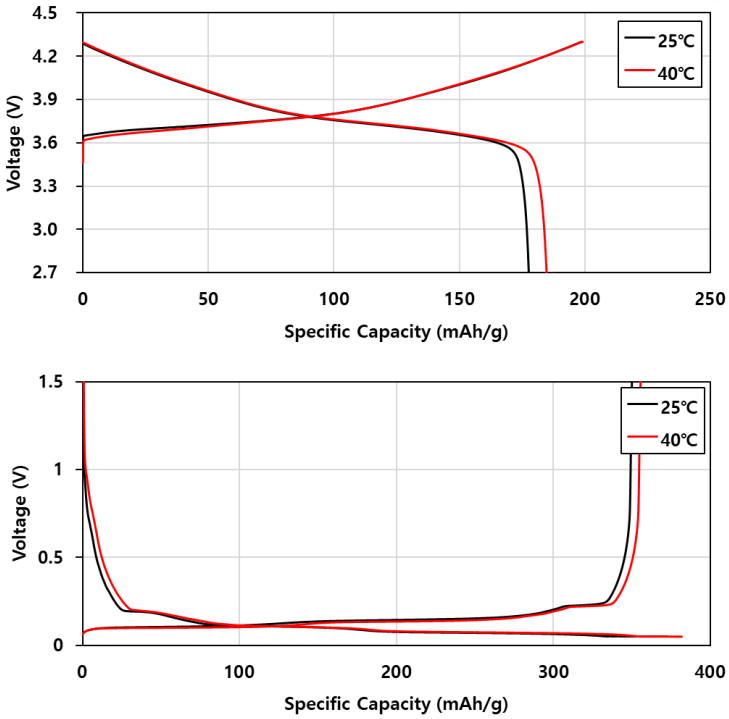

Figure 12. Formation cycle of NCM622, Graphite half-cell graph at 25℃ and 40℃

Table 8. Cathode, Anode half-cell formation cycle result

	Cathode		Anode	
	25℃	40℃	25℃	40℃
Specific charge capacity (CC / CC-CV) (mAh/g)	197.9/198.9	198.7/199.1	327.8/372.4	354.8/381.7
Specific discharge capacity (mAh/g)	177.6	184.7	350.0	355.5
Initial Coulombic efficiency (ICE)	89.3%	92.8%	94.0%	93.1%

3.4 NP ratio design at 40℃

Fig 13. is a graph that predicted the full cell formation cycle at 40℃ through the half-cell test result at 40℃. Compared with 25℃, it can be seen that the discharge of a full cell is an anode limit case in which discharge is terminated by consumption of Li charged in the negative electrode. And when comparing the design value with the actual result, it can be seen that the design through the half-cell result at 40℃ is more accurate. Changes in the reversible specific capacity and CE of the cathode and anode materials due to different temperatures change so that the limit design changes in the full cell.

Fig 14. show result of formation cycle of the full cell which was operated at 40℃. As expected, the discharge was terminated by the anode, because there is no more cyclable lithium inventory, so the anode potential was steeply increased at the end of the discharge. When comparing the capacity of the design and the actual cell, the charge capacity showed similar values, but the discharge capacity was lower than expected. This is because unwanted side reactions are also facilitating due to the increase in temperature. However, at the end of the discharge, the behavior of the potential of anode behaved as expected, so more accurate predictions would be possible by tuning other parameters.

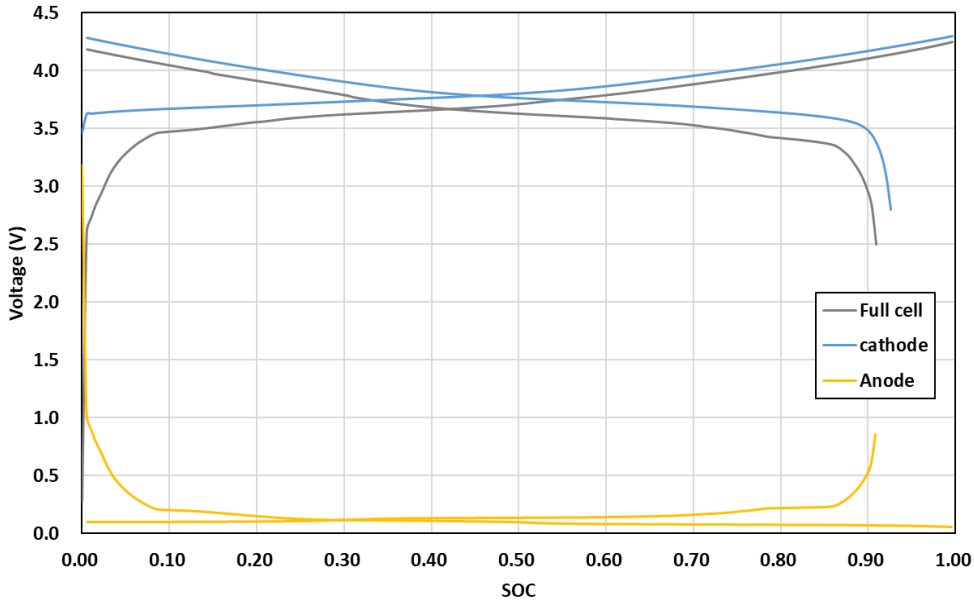

Figure 13. Predicted full cell plot through half-cell result at 40℃

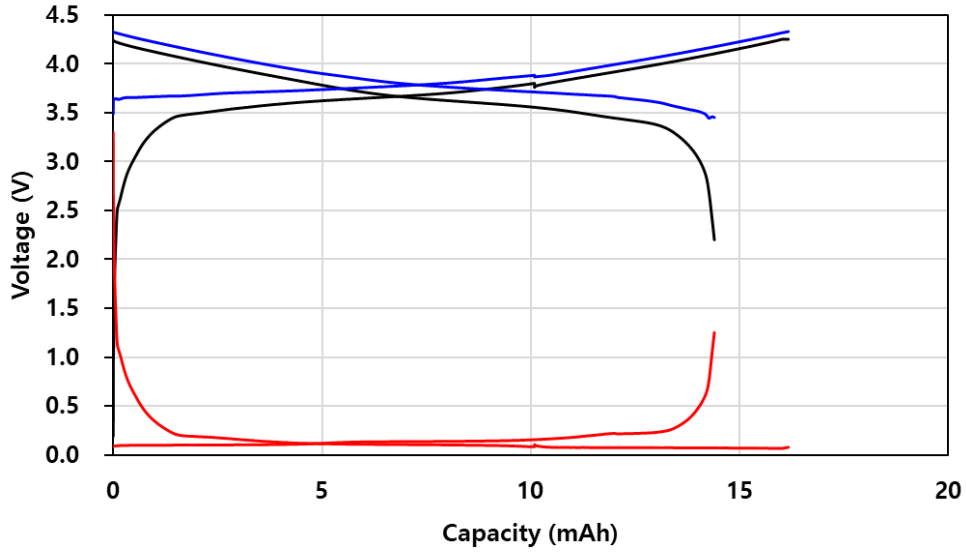

Figure 14. Formation cycle graph of NCM622/Graphite full cell operated at 40℃ and designed at 40℃

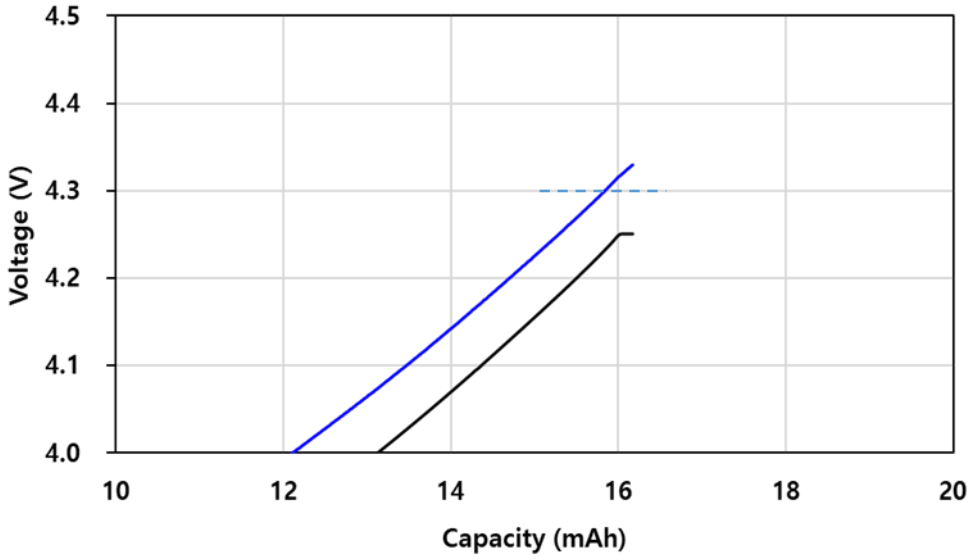

Figure 15. Formation cycle graph at the end of the charge of NCM622/Graphite full cell operated at 25℃

Table 9. NP ratio design of full cell at 25℃

	CC Charge NP	Charge NP	Discharge NP
Design	1.009	1.083	1.087

Table 10. Full cell formation cycle result at 25℃

	Charge capacity (mAh)	Discharge Capacity (mAh)	ICE
Design	16.04	14.62	91.2%
Real	16.17	14.40	89.1%

3.5 Temperature influence of NP ratio design

3.5.1 Formation cycle of full cell at 25℃ and 40℃ with 25℃ design

To see what difference the design temperature and operating temperature give between the predicted value and the actual value, the full cell formation cycle was carried out with different temperatures. **Fig 16.** is the result of designing at 25℃ and operating the formation cycle at 25℃ and 40℃ respectively. And their expected design values and actual results are indicated in **Table 10.** and **11.** The result of the full cell, which operated with the formation cycle at 25°C, quite similar to the predicted value, At the end of the discharge, the potential decrease of the cathode in the cell is the main reason that the voltage of the full cell reaches the discharge cut-off.

On the other hand, the case where the design and operating temperature are different is the case of 40℃ in **Fig 16.** Unlike 25 degrees, an increase in the voltage of the anode was observed at the end of the discharge, and the actual cell capacity was close to that predicted through the results of 40 degrees.

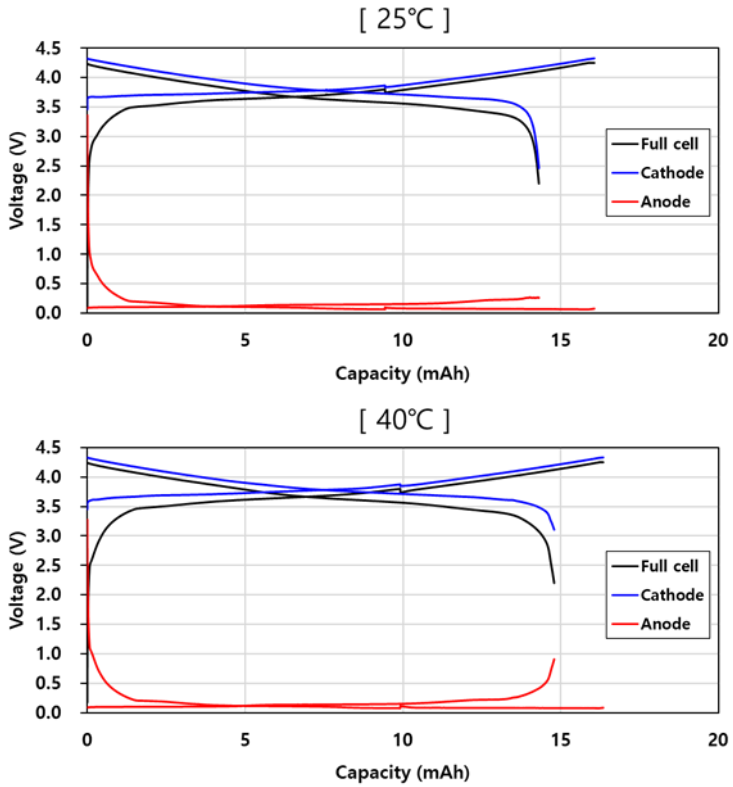

Figure 16. Formation cycle graph of full cell operated at 25℃ and 40℃ by designed 25℃

Table 11. Comparison between design and real cell (design at 25℃, operating at 25℃)

	Temperature (℃)	CC Charge NP	Charge NP	Discharge NP
Design	25	1.020	1.155	1.216
	40	1.100	1.181	1.164
	Temperature (℃)	Charge capacity (mAh)	Discharge capacity (mAh)	ICE
Design	25	15.80	14.11	89.3%
	40	15.82	14.29	90.4%
Real	25	16.06	14.31	89.1%

Table 12. Comparison between design and real cell (design at 25℃, operating at 40℃)

	Temperature (℃)	CC Charge NP	Charge NP	Discharge NP
Design	25	1.002	1.134	1.194
	40	1.080	1.159	1.164
	Temperature (℃)	Charge capacity (mAh)	Discharge capacity (mAh)	ICE
Design	25	15.80	14.11	89.3%
	40	16.05	14.54	90.5%
Real	40	16.34	14.79	90.5%

3.5.2 Formation cycle of full cell at 25℃ and 40℃ with 40℃ design

Fig 17. is the result of designing at 25℃ and operating the formation cycle at 25℃ and 40℃ respectively. And their expected design values and actual results are indicated in **Table 12**. and **13.** When the formation cycle was performed at 25℃, the result was more similar to the expected value of 25℃ than the expected of 40℃. This can be confirmed in the graph of the full cell. In a cell at 40℃, an increase in the voltage at the anode is expected to cause the discharge to end in the full cell. Capacity and efficiency were also closer to the same temperature design.

The result of a cell operated at 40℃ seems to follow the design of 25℃ for capacity and efficiency values, but it is not. Looking at the graph of 40℃ in **fig 17.**, it follows the case of anode limit, not cathode limit design of 25℃. Discharge capacity and efficiency lower than the design are expected to be caused by an increase in unwanted side reactions with increasing temperature.

When the operating temperature is different from the design temperature, it can be confirmed that there is a difference in the charge/discharge voltage behavior predicted by the design. Even the type of electrode that causes the cell voltage to reach the cut-off voltage has changed. This unexpected voltage behavior can lead to unwanted degradation.

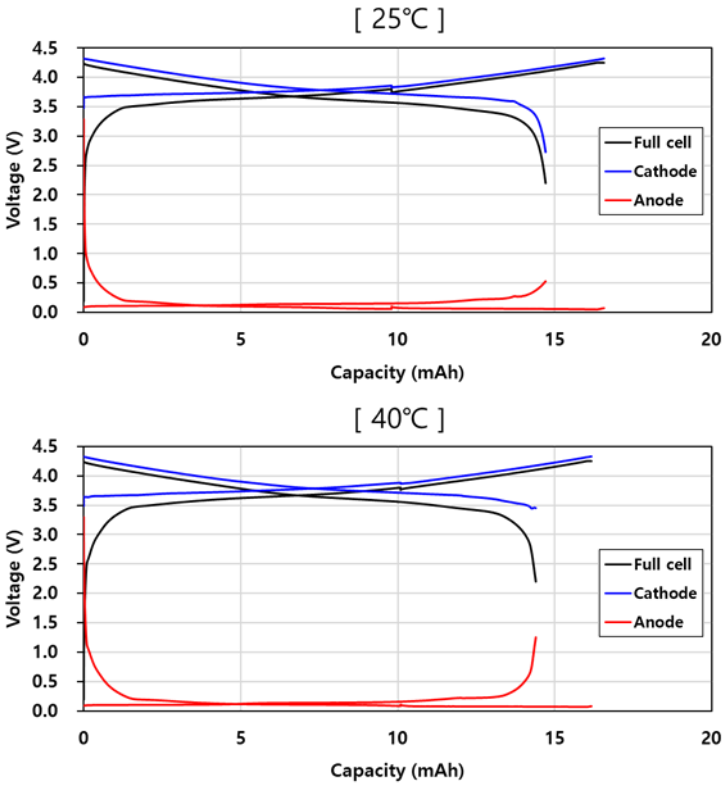

Figure 17. Formation cycle graph of full cell operation at 25℃ and 40℃ by designed at 40℃

Table 13. Comparison between design and real cell (design at 40℃, operating at 25℃)

	Temperature (℃)	CC Charge NP	Charge NP	Discharge NP
Design	25	0.926	1.048	1.103
	40	0.998	1.071	1.075
	Temperature (℃)	Charge capacity (mAh)	Discharge capacity (mAh)	ICE
Design	25	16.43	14.67	89.3%
	40	16.44	15.00	91.3%
Real	25	16.57	14.71	88.8%

Table 14. Comparison between design and real cell (design at 40℃, operating at 40℃)

	Temperature (℃)	CC Charge NP	Charge NP	Discharge NP
Design	25	0.936	1.059	1.116
	40	1.009	1.083	1.087
	Temperature (℃)	Charge capacity (mAh)	Discharge capacity (mAh)	ICE
Design	25	16.02	14.31	89.3%
	40	16.04	14.62	91.2%
Real	40	16.17	14.40	89.0%

IV. Conclusion

In order to see the effect of temperature in the design of the NP ratio, half-cell and full cell formation cycles were conducted at 25℃ and 40℃ and compared. In addition, in order to accurately measure the capacitance and observe the behavior of the voltage, a three-electrode system was used that introduced a reference electrode located where the electrode and the electrode face each other.

Since the charge, discharge capacity, and initial Coulombic efficiency of the cathode and the anode are different at 25℃ and 40℃, the full cell must be designed using the half-cell test result at the same temperature as the operating temperature.

The difference between the design temperature and the operating temperature results in a difference between the expected Anode and cathode voltage behavior in a full cell design. So, the temperature must be considered in the cell design.

V. Reference

1. Ding, Y., Cano, Z. P., Yu, A., Lu, J., & Chen, Z. (2019). Automotive Li-ion batteries: current status and future perspectives. Electrochemical Energy Reviews, 2(1), 1-28.
2. Chen, C. H., Planella, F. B., O'Regan, K., Gastol, D., Widanage, W. D., & Kendrick, E. (2020). Development of Experimental Techniques for Parameterization of Multi-scale Lithium-ion Battery Models. Journal of The Electrochemical Society, 167(8), 080534.
3. Zhou, J., & Notten, P. H. L. (2004). Development of reliable lithium microreference electrodes for long-term in situ studies of lithium-based battery systems. Journal of the Electrochemical Society, 151(12), A2173.
4. Tornheim, A., & O'Hanlon, D. C. (2020). What do Coulombic Efficiency and Capacity Retention Truly Measure? A Deep Dive into Cyclable Lithium Inventory, Limitation Type, and Redox Side Reactions. *Journal of The Electrochemical Society*, *167*(11), 110520.
5. Zhou, H., Xin, F., Pei, B., & Whittingham, M. S. (2019). What limits the capacity of layered oxide cathodes in lithium batteries?. *ACS Energy Letters*, *4*(8), 1902-1906.
6. Kasnatscheew, J., Evertz, M., Streipert, B., Wagner, R., Klöpsch, R., Vortmann, B., ... & Lamp, P. (2016). The truth about the 1st cycle Coulombic efficiency of LiNi 1/3 Co 1/3 Mn 1/3 O 2 (NCM) cathodes. *Physical chemistry chemical physics*, *18*(5), 3956-3965.
7. Bhattacharya, S., Riahi, A. R., & Alpas, A. T. (2014). Thermal cycling induced capacity enhancement of graphite anodes in lithium-ion cells. *Carbon*, *67*, 592-606.

VI. Acknowledgement

Special thanks to dissertation committee assistant referees, Prof. Hyun-Kon Song and Prof. Dong-Hwa Seo.

Lastly, I sincerely appreciate Prof. Kyeong-Min Jeong.